Eur Biophys J (1999) 28: 552–563

ARTICLE

Oxana R. Dobrovinskaya · Jesus Muñiz
Igor I. Pottosin

Asymmetric block of the plant vacuolar Ca^{2+}-permeable channel by organic cations

Received: 22 February 1999 / Revised version: 6 July 1999 / Accepted: 8 July 1999

Abstract In this work we have analysed the voltage-dependent block of the slow activating channel from red beet vacuoles by Tris, quaternary ammonium ions and the natural polyamines putrescine, spermidine and spermine. All these organic cations when applied from the cytosolic side blocked the channel by binding apparently deep ($z\delta$ values in the range of 0.65–1.35) within the pore. Tetraethylammonium ion did not pass the selectivity filter, whereas the cations with a smaller cross-section and Tris could pass across the entire pore, as evidenced by a relief of block at high positive voltages. Voltage dependence of the establishment of block from cytosolic side and of its relief was anomalously strong in the sense that the total charge moved across the pore for all blockers tested, with a notable exception of spermine, was in excess of their actual valence. This behaviour is consistent with the existence of multiple binding sites within a long pore, their simultaneous occupancy and interaction between different ions. In contrast, binding of blockers from the vacuolar (lumenal) side appears to follow a single-ion handling rule, with a common binding site for all amines located at approximately 30% of the electrical distance from the lumenal side.

Key words Voltage-dependent block · Quaternary ammonium · Polyamines · Tris · Slow vacuolar channel

Introduction

Except for K^+-selective channels of higher plant plasma membranes (Hedrich et al. 1995; Czempinski et al. 1997; Dreyer et al. 1997) which share structural motifs with their counterparts in animal cells, little is known on the structural design of other plant ion channels, including those well characterised by means of electrophysiological techniques. The so-called SV (for Slow Vacuolar) channel is a ubiquitous component of vacuolar endomembranes of higher plant cells (Hedrich et al. 1988). The SV channel conducts both mono- and divalent cations but is not measurably permeable for small monovalent anions (Pantoja et al. 1992; Ward and Schroeder 1994). It is gated open by high cytosolic Ca^{2+} and a cytosol-positive membrane voltage (Hedrich and Neher 1987). Because of its Ca^{2+} permeability and of the activation by cytosolic Ca^{2+}, it was proposed that the SV channel, similarly to the ryanodine receptor channel from animal cells, mediates Ca^{2+}-induced Ca^{2+} release from the vacuole (Ward and Schroeder 1994). This function seems to be limited, however, owing to the down regulation of the SV channel by Ca^{2+} from the lumenal side, so the gate is predominantly closed by a cytosol-directed electrochemical gradient for Ca^{2+} (Pottosin et al. 1997).

Previous studies of the effects of various organic and inorganic blockers on the SV channel revealed a peculiar pharmacological pattern, as it was sensitive to the blockers of the anion channels (Zn^{2+}, DIDS, ethacrinic acid, A-9-C) as well as to those of the cationic ones [e.g. charibdotoxin, quinine, quinacrine, TEA^+(TEA = tetraethylammonium) tubocurarine] (Hedrich and Kurkdjian 1988; Weiser and Bentrup 1993). Thus, the SV channel could not be easily arranged into any known ion channel category, and a structural basis for its selective permeability remained elusive (Allen et al. 1998). In the present work we have probed the gross architecture of the channel pore by various organic blockers.

The first attempt at the evaluation of the length of the constriction region within a pore came from analysis of the voltage dependence of the SV channel block by linear polyamines (Dobrovinskaya et al. 1999). This evaluation was originally based on a similar approach elaborated by Miller (1982) and further utilised by

O.R. Dobrovinskaya · J. Muñiz · I.I. Pottosin (✉)
Centro Universitario de Investigaciones Biomedicas,
Universidad de Colima,
28047 Colima, Col., México
e-mail: pottosin@cgic.ucol.mx

others (Tinker and Williams 1995; Villarroel et al. 1988). The principle underlying the measurement of the physical distance of the voltage drop within the channel pore was to use bis-quaternary ammonium ions (or polyamines in our work) of different lengths as molecular calipers. The first group marked a certain blocking position within a channel pore, whereas the other(s) is (are) positioned at varying locations within the voltage drop, depending on the blocker length, which is monitored by a change of the voltage dependence of the block ($z\delta$). This approach, however, could be used only for the pores handling one ion at a time, where the $z\delta$ value unequivocally reflects the interaction of a single blocking ion with a pore. There were indications that the SV channel behaved as a multi-ion pore (Gambale et al. 1996), although the block by cytosolic polyamines under the experimental conditions of our previous study seemed to follow a simple one-to-one binding mechanism. However, it was found here that the multi-ion nature of the polyamine block, which would invalidate our previous analysis, was masked by the presence of $Tris^+$ [Tris = tris(hydroxymethyl)aminomethane], which itself turned out to block the SV channel in a complex manner. Therefore we have modified our approach, now studying $Tris^+$ and polyamine effects separately and referring to a total charge transported across the pore upon the blocking-unblocking reaction (z) rather than to the voltage dependence of block ($z\delta$) only. In addition, to unravel the asymmetric location of the principle energy barrier (tentative selectivity filter) within the pore, a more direct approach was addressed, by testing blocking ions also from the vacuolar side and by comparison of the resulting voltage dependence with that obtained for the block from the cytosolic side. Another goal of the present work was to estimate the calibre of the narrowest cross-section within the SV channel pore. To do that, we have tested the capability of quasi-spherical quaternary ammonium ions and $Tris^+$ to permeate across the entire pore. A preliminary report of this work has been presented in abstract form (Pottosin et al. 1999).

Materials and methods

Isolation of vacuoles, patch-clamp media and recording

Fresh *Beta vulgaris* (whole plants) were received twice a week from a local market and kept at +4 °C before use. Vacuoles were isolated mechanically as described previously (Dobrovinskaya et al. 1999) and resuspended at +25 °C in a basic solution containing (in mM): 100 KCl, 2 $CaCl_2$, 450 sorbitol, 15 Hepes-KOH (pH 7.5). For patch-clamp recording the bath solution was substituted by another one containing 100 μM free Ca^{2+}. Previous analysis has shown that up to 40% of available SV channels could be activated under these conditions (Dobrovinskaya et al. 1999). At 100 μM free Ca^{2+} the single SV channel current was blocked by 20% at the most at high positive voltages. Higher concentrations of Ca^{2+} caused larger degrees of block (Pottosin et al. 1999) whereas at lower concentration a stable activity of a SV channel could not be maintained. The patch pipette filling solution, if not indicated, was the same as the aforementioned basic solution but with 5 mM EGTA instead of 2 mM $CaCl_2$ (free Ca^{2+} about 2 nM). All chemicals were analytical grade (Sigma, St Louis, Mo.).

Fabrication and parameters of patch-pipettes were as described previously (Dobrovinskaya et al. 1999). The measurements of vacuolar ion currents were done on isolated tonoplast patches in an outside-out (cytoplasmic side of the membrane faces the bath) configuration using an Axopatch 200A integrating patch-clamp amplifier (Axon Instruments, Foster City, Calif.). The convention of current and voltage was as follows: the sign of the voltage refers to the cytosolic side, and positive (outward) currents represent a flux of cations into the vacuole. Single channel currents were filtered at 2 kHz by a low-pass Bessel filter, sampled at 10 kHz, and recorded directly on a hard disk of an IBM-compatible PC.

Voltage protocol

The command voltage protocols were applied and the analyses were carried out using the pClamp 6.0 software package (Axon Instruments, Foster City, Calif.). Unitary current-voltage relationships of the SV channel were analysed in a continuous manner using ramp-wave voltage protocols as described previously (Dobrovinskaya et al. 1999). The ramp duration of 12.5 or 25 ms was chosen, as it was normally short enough to conserve the SV channel either open or closed depending on its state at the beginning of the pulse. To obtain the single-channel current-voltage relationship, currents were corrected for the leak and capacitance simply by subtracting the averaged responses containing no channel openings. To increase the signal-to-noise ratio, many individual I/V relationships were averaged.

Theory

To describe the voltage dependence of a block a conventional double barrier-one well (binding site) model of a voltage-dependent block was used (Woodhull 1973; Hille 1992). Generally, the permeation of the blocking cation was considered; hence the state diagram for the cation processing across the channel pore from the *cis* to the *trans* side was as follows:

$$E + [B]_{cis} \underset{k_b}{\overset{k_f}{\rightleftharpoons}} E^*[B] \xrightarrow{k} E + [B]_{trans} \quad (1)$$

where E and E*[B] are unblocked and blocked channel states, respectively. Because the cations were added from

the *cis* (cytosolic or vacuolar) side only, the reversal of the second step, in full analogy with the well-known Michaelis-Menten model, was not considered. Assuming a symmetrical shape of the barriers and of the well (Hille 1992), the voltage dependence of the forward (k_f), backward (k_b) and "catalytic" (k) rate constants can be expressed as follows:

$$k_f = k_f(0) \times \exp(z\delta \times VF/2RT)$$
$$k_b = k_b(0) \times \exp(-z\delta \times VF/2RT) \quad (2)$$
$$k = k(0) \times \exp(z(1-\delta) \times VF/2RT)$$

where $k_f(0)$, $k_b(0)$, $k(0)$ are the values of the corresponding rate constants at 0 mV, z is the effective blocking charge, δ is the fraction of the membrane electrical field left behind the blocking cation on its movement to the binding site within the channel pore (for long multivalent ions, δ reflects a mean displacement of charges within the electric field), V is the membrane voltage, and F, R and T have their usual meanings. Using Eqs. (1) and (2), substituting k_f/k by k_1 and k_b/k by k_2, and assuming that the blocked state E*[B] is non-conducting, one obtains the ratio of the current in the presence of the blocking cation to the current in the control as a function of the membrane voltage and of the blocker concentration, [B]:

$$I_{(+B)}/I_{control} = \left[1 + \frac{k_1(0) \times [B] \times \exp(z\delta \times VF/RT)}{k_2(0) + \exp(z \times VF/2RT)}\right]^{-1} \quad (3)$$

It can be easily seen from this formula that if $k_b(0) \gg k(0)$, a half-blocking concentration at 0 mV will be equal to the dissociation constant, $K_d(0) = k_2(0)/k_1(0)$. A trivial case of an impermeable blocker, i.e. with $k(0) = 0$, results in a simplified expression:

$$I_{(+B)}/I_{control} = [1 + (k_1(0)/k_2(0)) \times [B] \times \exp(z\delta \times VF/RT)]^{-1} \quad (4)$$

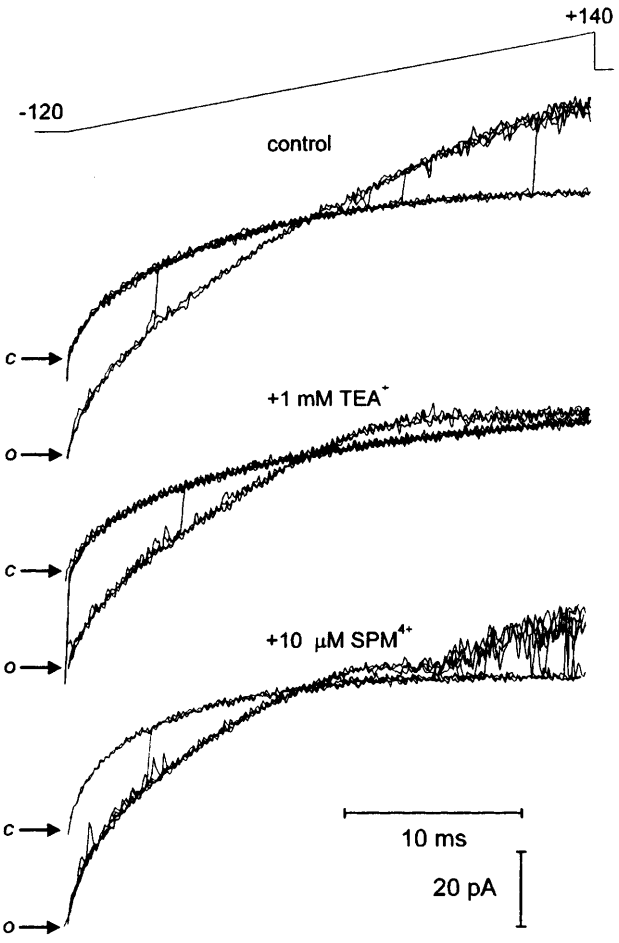

Fig. 1 Examples of unitary current-voltage relationships of the SV channel in the cytosolic side-out patch of the vacuolar membrane of *Beta vulgaris*. Single channel currents were elicited by a ramp-wave voltage protocol given at the top. Original records were filtered at 2 kHz and sampled at 10 kHz. Symbols *o* and *c* indicate open and closed (leak current) channel levels, respectively. For illustrative purposes the traces with transitions between closed and open states, normally removed during analysis, are preserved. Pipette and bath solutions contained symmetrical 100 mM KCl, 15 mM Hepes-KOH (pH 7.5). Pipette contained 5 mM EGTA (~2 nM free Ca^{2+}), bath Ca^{2+} buffer with free Ca^{2+} concentration 100 μM (control). Blockers, 1 mM tetraethylammonium chloride (TEA^+) and 10 μM spermine · 4HCl (Spm^{4+}), were applied to the cytosolic side of the patch by bath perfusion

Results

General observations

Examples of single channel recordings in the absence or presence of blocking cations, in this case tetraethylammomium (TEA^+) and spermine, at one membrane side are shown in Fig. 1. As can be seen, blockers applied from cytosolic side have almost no effect on the inward single channel current, whereas the outward current is suppressed in a voltage-dependent manner, a progressive decrease in the case of TEA^+ and a decrease followed by an upturn of the open channel current in the case of spermine. The effective concentrations of blockers used in this work varied from micromolar for spermine and spermidine through submillimolar to low millimolar for putrescine up to millimolar for TEA^+, TMA^+ and $Tris^+$. The blocking events in the case of blockers effective at millimolar concentrations were too fast to be resolved by our equipment, so the apparent reduction of the single channel current was not accompanied by a measurable increase of the open channel current noise (Fig. 1, +1 mM TEA). In contrast, blockers effective at micromolar concentrations caused a flickering of the open channel current or even partly resolved (submillisecond) interruptions (Fig. 1, +10 μM spermine). Although in this case the kinetics of the block could be in principle studied directly, we have restricted ourselves to measurements of the mean open channel current which was achieved by averaging many individual current-voltage relationships as the ones presented in Fig. 1.

Block of the SV channel by quaternary ammonium ions and Tris

The effects of small tetraalkylammonium ions, tetramethylammonium (TMA^+) and TEA^+, on the single channel current were first tested from the cytosolic side. Application of 10 mM of TMA^+ or TEA^+ reduced the open channel current in a strongly voltage-dependent manner (Fig. 2a, b). The effect of TMA^+ and TEA^+ was different as TEA^+ at large positive potentials reduced the current to the vanishing small level whereas the relative current in the presence of TMA^+ appeared to approach a plateau, as if TMA^+ had a small but significant permeability. To test this hypothesis quantitatively we have fitted the relative open channel currents in the presence of TMA^+ and TEA^+ by either a permeable or impermeable blocker model, described by Eqs. (3) and (4), respectively (Fig. 2b). In the case of TMA^+, a permeable blocker model fits the data substantially better (F-test 1.25×10^{-12}), whereas in case of TEA^+ with a probability of 0.99 no preference could be given to either of the two models. In the experiment presented in Fig. 2a, b the voltage dependence of the block has been analysed over a wide range of potentials, so the relief of the block by TMA^+ could be studied in detail. When we attempted to fit the whole dependence, fixing the effective blocking charge, z, to the actual valence of TMA^+, $+1$, the fit did not explain adequately the last portion of the voltage dependence at high positive potentials (not shown). At the next step we handle z as a free running parameter. The resulting fit described the data points in Fig. 2b substantially better (for $z \equiv 1$ versus z free, the F-test gave 0.01), yielding $z = 1.48$. We have analysed the voltage dependence of the block by TMA^+ (concentrations 1, 3 and 10 mM) on four separate patches. No significant concentration dependence of the blocking parameters was observed. The mean of z was 1.70 ± 0.07 at 1 mM and 1.60 ± 0.12 at 10 mM; the average electrical distance, δ, was 0.64 ± 0.05 ($z\delta = 0.96 \pm 0.04$). The constants $k_1(0)$ and $k_2(0)$ for 10 mM (1 mM) were $2.35 \pm 0.52 \times 10^2$ ($1.98 \pm 0.40 \times 10^2$) M^{-1} and 13 ± 3 (12 ± 2), respectively, yielding an average $K_d(0)$ of $5.8 \pm 0.3 \times 10^{-2}$ M. Analysis of the voltage dependence of the block by TEA^+ (concentrations 1, 3 and 10 mM, each tested on three separate patches), using Eq. (4) for an impermeable blocker, yielded an average K_d at zero voltage of $1.2 \pm 0.2 \times 10^{-2}$ and $z\delta = 0.94 \pm 0.08$. Thus, the steepness of voltage dependence was the same as with TMA^+, but TEA^+ binds with approximately five times higher affinity compared to TMA^+.

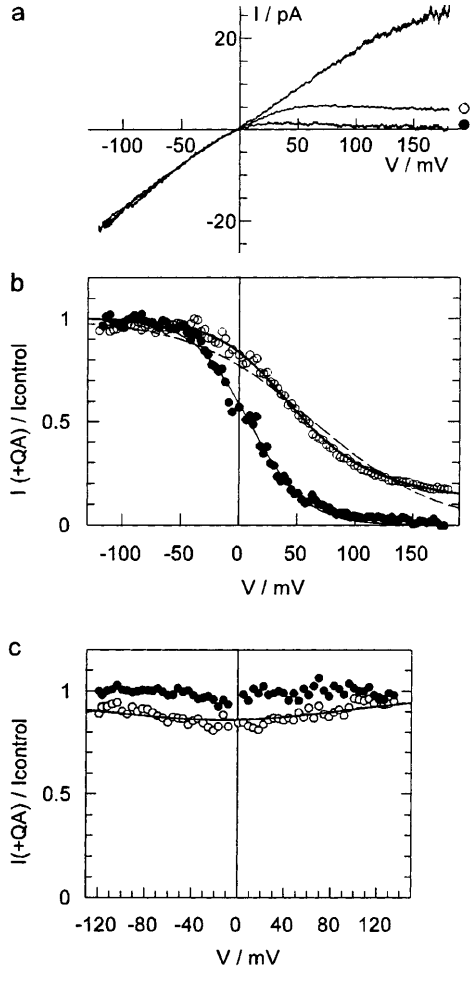

Fig. 2a–c Effect of quaternary ammonium ions on the open channel current-voltage relationship. **a** Single SV channel current voltage-relationship (n, number of individual curves averaged) at control conditions (symmetrical 100 mM KCl, $n = 43$) and in the presence of 10 mM of TMA (○, $n = 43$) and TEA (●, $n = 35$) at the cytosolic side of the patch. **b** Corresponding relative currents (in the presence of blocker to control) as a function of voltage. The number of points was reduced three times by substitutive average. The *dashed line* is the best fit by Eq. (4) assuming the impermeability of the blocker; for TMA an alternative fit by Eq. (3), assuming weak permeability of the blocker and valence, z, as a variable, is presented (*thick line*). **c** Block by 10 mM TMA ($n = 27$) or TEA ($n = 49$) applied to the vacuolar side. Relative current for TMA is fitted to Eq. (3), $z = 1$ (*solid line*). The mean relative current in the presence of TEA was 0.99 ± 0.036 of that in the control

So far as TMA^+ was considered to be a permeable blocker when applied from the cytosolic side, whereas TEA^+ permeation was undetectable, it was intriguing to test the effects of these components from the opposite membrane side. The results of representative experiments with 10 mM TEA^+ or TMA^+ at the vacuolar side are shown in Fig. 2c (three separate patch pipettes containing either control solution or one with 10 mM of blocker were used for measuring I/V relationships on the same vacuolar sample). It can be seen that TEA^+ was completely ineffective, whereas TMA^+ displayed a transient block, the most prominent at zero voltage. Fit of data points for TMA^+ by Eq. (3) ($z \equiv 1$) yielded $k_1(0) = 3.8 \times 10^1$ M^{-1}, $k_2(0) = 1.5$ [$K_d(0) = 4.0 \times 10^{-2}$ M] and the electrical distance to the binding site, $\delta = 0.28$.

For the next series of experiments we took another amine, Tris, which has a size of approximately that of TEA^+. Block by $Tris^+$ from the cytosolic side qualita-

tively resembles that of TMA^+ (Fig. 3a, c). The difference was that the upturn of current, reflecting the block relief at high positive potentials, was expressed more clearly compared to that in the presence of TMA^+ (Fig. 2b). Fits of the data points in Fig. 3c by model of the permeable blocker [Eq. (3)] with fixed $z = 1$ were not consistent. Treatment of z as a free-running parameter resulted in an adequate description of the experimental voltage dependence of the block. Parameter z showed moderate concentration dependence, decreasing from 2.26 ± 0.03 at 10 mM $Tris^+$ to 1.72 ± 0.07 at 56 mM $Tris^+$ ($n = 3$ separate patches). Thus, the block by monovalent $Tris^+$ resembles that produced by a divalent blocker at all concentrations tested (fit of single experiment with 3 mM $Tris^+$ at cytosolic side revealed $z = 2.35$). The apparent electrical distance to the binding site, δ, did not change significantly with concentration, 0.37 ± 0.04 and 0.38 ± 0.04 at 10 and 56 mM $Tris^+$, respectively ($\delta = 0.39$ at 3 mM $Tris^+$). Consequently, the voltage dependence of the block decreased with the increase of concentration of blocker; $z\delta$ changed from 0.92 to 0.65 by changing the $Tris^+$ concentration from 3 mM to 56 mM. The energy profile of the cytosolic part of the pore, i.e. the depth of the well and relative heights of the energy barriers, appeared to be quite similar for $Tris^+$ and TMA^+. For $Tris^+$ concentrations of 10 mM and 56 mM we obtained the values for constants $k_1(0) = 5.1 \pm 1.5 \times 10^2\ M^{-1}$ and $2.9 \pm 0.7 \times 10^2\ M^{-1}$, $k_2(0) = 27 \pm 7$ and 18 ± 10, yielding a $K_d(0)$ of $5.9 \pm 1.2 \times 10^{-2}$ M and $5.7 \pm 1.2 \times 10^{-2}$ M, respectively.

Finally, we have tested the blocking effects of $Tris^+$ from the vacuolar side. A typical experiment is shown in Fig. 3b, d. We have expected that $Tris^+$, if it blocks the channel from the opposite side of the pore, has to be removed to the cytosolic side at large negative potentials. When applied from the vacuolar side, $Tris^+$ showed a shallower voltage dependence of the block compared to that of the cytosolic application. To prove that $Tris^+$ permeates we had to decrease the voltage down to the largest attainable negative value, −220 mV; more negative potentials usually broke the patch before any meaningful measurement had been started. The effective concentration of $Tris^+$ from the vacuolar side was also higher compared to that from the cytosolic one, so the fits of the relative currents in Fig. 3d by two alternative models expressed by Eqs. (3) and (4) showed only a marginal difference at $Tris^+$ concentrations of 10 and 28 mM. However, at 56 mM vacuolar $Tris^+$ the trend of the upturn of the relative current became obvious in the examined range of potentials [the probability that the fits given by Eqs. (3) and (4) are the same dropped below 5%]. We have summarised the analytical results on three patches with 10 mM $Tris^+$ at the vacuolar side, two other

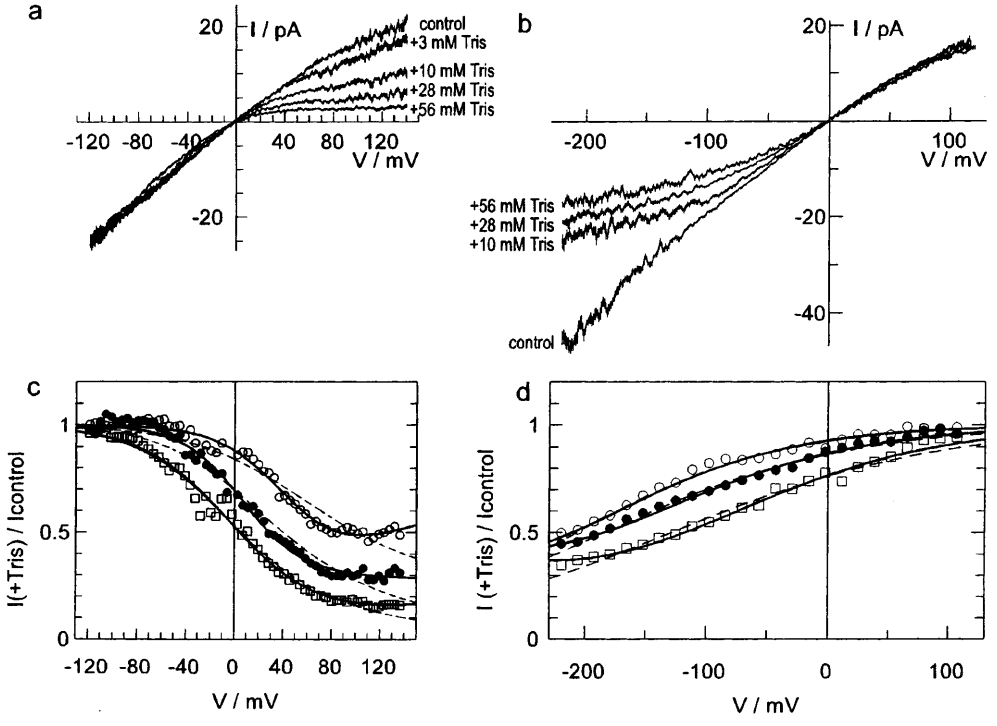

Fig. 3 Effect of cytosolic (**a**, **c**) and vacuolar (**b**, **d**) $Tris^+$ on the single SV channel current-voltage relationship. Number of individual current-voltage relations used for each curve (mean ± SD) was: **a** control ($n = 15$), $Tris^+$: 3 mM ($n = 17$), 10 mM ($n = 19$), 28 mM ($n = 16$), 56 mM ($n = 38$); **b** control ($n = 33$), $Tris^+$: 10 mM ($n = 46$), 28 mM ($n = 49$), 56 mM ($n = 47$). **c**, **d** Corresponding relative currents as a function of voltage for 10 mM $Tris^+$ (*open circles*), 28 mM $Tris^+$ (*filled circles*) and 56 mM $Tris^+$ (*squares*); the number of points was reduced 5 or 12 times by substitutive average. The data points in **c** were fitted to Eq. (3) assuming fixed valence $z = 1$ for $Tris^+$ (*dashed lines*) or by incorporating the valence as a free running parameter (*thick lines*). In **d** the data were fitted by Eq. (3) (*thick lines*) or by Eq. (4) (*dashed lines*) assuming that $Tris^+$ is either a permeable or impermeable blocker, respectively; the valence (z) for all fitted curves was fixed to 1

patches with 28 mM vacuolar $Tris^+$ and three further patches exposed to 56 mM $Tris^+$ at the vacuolar side. The apparent $K_d(0)$ hardly changed with concentration, $1.81 \pm 0.50 \times 10^{-1}$ M and $1.81 \pm 0.48 \times 10^{-2}$ M at 10 and 56 mM $Tris^+$, respectively, or approximately three times lower affinity compared to that from the cytosolic side. This was caused mainly by the increase of $k_2(0)$ (mean value of 127 ± 25) which was only partly compensated by the increase of $k_1(0)$ [$k_1(0) = 6.1 \pm 1.4 \times 10^2$ M^{-1}]. This implies that the binding site for $Tris^+$ from the lumenal side is shallower compared to the cytosolic one, whereas the energy barriers at the entrance have similar heights. The binding of $Tris^+$ from the vacuolar side appeared to follow a simple 1:1 binding scheme, without any evidence for multi-ion occupancy. We tried to describe the data by Eq. (3) with variable z; however, this did not improve the fits and yielded z values in the range of 0.98–1.06, which did not differ significantly from the actual valence of $Tris^+$ (result not shown). Therefore, the voltage dependence has been fitted by fixing z to 1.0, yielding the apparent electrical distance to the binding site, δ, from the vacuolar side of 0.33 ± 0.03, 0.30 ± 0.01 and 0.29 ± 0.01 for 10, 28 and 56 mM $Tris^+$, respectively. Taking these results together with the invariance of $K_d(0)$, we have concluded that $Tris^+$ binds to a single site, which is located at about 30% of the voltage difference across the pore from the vacuolar side.

Block of the SV channel by polyamines

We have showed previously that natural polyamines, putrescine (Put^{2+}), spermidine (Spd^{3+}) and spermine (Spm^{4+}), potently blocked the current through the SV channel from the cytosolic side (Dobrovinskaya et al. 1999). However, these results have been obtained in the presence of 28 mM $Tris^+$ as a part of pH-buffer system. It just has been shown in the present work that $Tris^+$ itself blocks the channel in a complex manner. Thus, there was a need for re-evaluation of the polyamine block in the absence of other blocking cations.

Examples of single channel current-voltage relationships obtained on the same cytosolic-side-out membrane patch in the presence of different concentrations of Put^{2+} and Spm^{4+} are shown in Fig. 4a, b, and the currents for three selected concentrations of each blocker taken relative to the open channel current in the control are plotted below (Fig. 4c, d). In the presence of polyamines the current-voltage relationship becomes N-shaped. At negative potentials it does not differ significantly from the control, being roughly linear. At positive potentials, first the region of negative conductance is observed, implying a steep increase of block, whereas at high positive potentials the current turns up, tending to approach the control level. Thus, polyamines appear to act as permeable blockers. The voltage dependence of the block at first glance looked quite similar for divalent Put^{2+} and tetravalent Spm^{4+}. We first attempted to fit the data points obtained with Put^{2+} by Eq. (3), fixing z to 2.0. As can be seen from Fig. 4c, this did not result in a reasonable description of the observed voltage dependence, although the data points could be fairly well fitted considering a variable z. For this experiment the successful fits yielded z in the range of 3.6–4.3, or roughly double the Put^{2+} valence. For Spm^{4+} the data points could be well described by z in the range of 3.7–

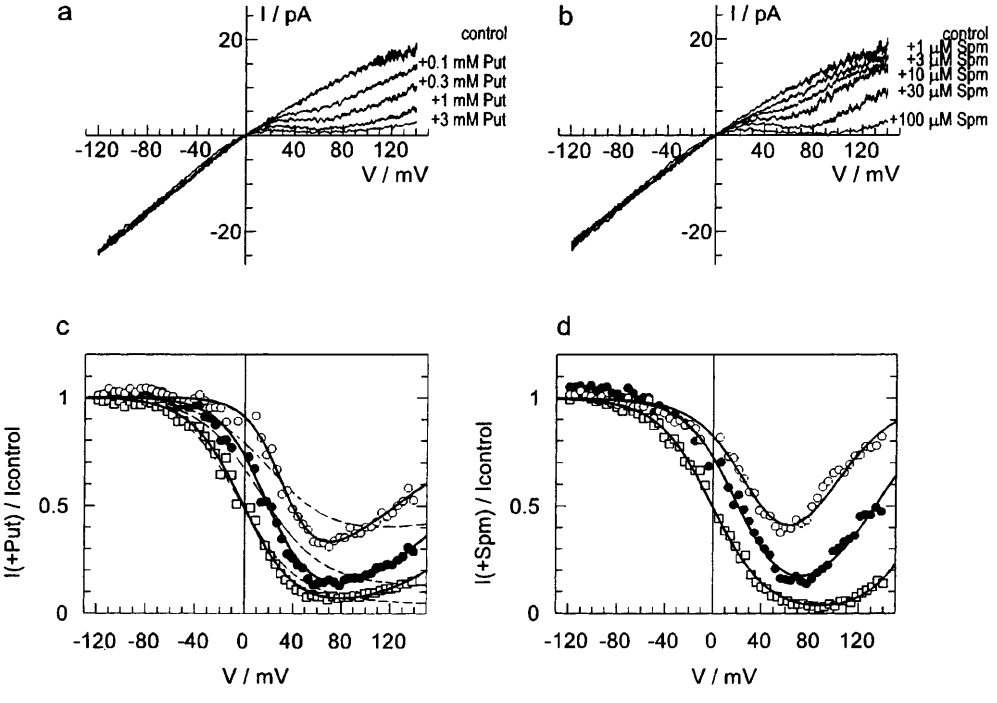

Fig. 4 Effects of cytosolic putrescine (**a**, **c**) and spermine (**b**, **d**) on the unitary SV current-voltage relation. Number of averaged individual curves in **a** was: control ($n = 29$), putrescine (Put) 0.1 mM ($n = 36$), 0.3 mM ($n = 24$), 1 mM ($n = 28$) and 3 mM ($n = 39$); and in **b** was: control ($n = 43$), spermine (Spm) 1 µM ($n = 54$), 3 µM ($n = 48$), 10 µM ($n = 26$), 30 µM ($n = 29$) and 100 µM ($n = 39$). **c**, **d** Corresponding relative currents; number of points was reduced five times by substitutive average; 0.3 mM Put or 10 µM Spm (*open circles*), 1 mM Put or 30 µM Spm (*filled circles*) and 3 mM Put or 100 µM Spm (*squares*) were fitted by Eq. (3) (*thick lines*) considering the effective valence of block, z, as a free running parameter. In **c** the data points were fitted for comparison by fixing the effective valence of the block to the actual valence of putrescine, $z = 2$ (*dashed lines*)

4.5 for the experiment presented in Fig. 4. We have summarised several experiments similar to that presented in Fig. 4. Parameters of the voltage-dependent block by Put^{2+}, Spd^{3+} and Spm^{4+} (mean ± SD) are collected in Table 1. As can be seen, the apparent dissociation constants for polyamines increased with the increase of concentration. For a 10-fold increase of concentration the binding affinity decreased 1.6 times for Put^{2+}, 2.4 times for Spd^{3+} and 2.3 times for Spm^{4+}. The apparent changes of binding of various polyamines with concentration could be fairly simulated by the introduction of an additional variable added up to the applied potential (result not shown). This shift, however, could not be explained by a reduction of membrane surface potential by the polyamines as, paradoxically, it was in the opposite direction. This is particularly evident from Fig. 4d, where the minima of the curves are shifted to more positive potentials with the increase of Spm^{4+} concentration at the cytosolic side, as if Spm^{4+} increased the membrane surface potential at the side of application. Also vice versa, when Spm^{4+} was applied to the vacuolar side, a negative shift of the minima with an increase of Spm^{4+} concentration was observed (Fig. 5d).

Surprisingly, the voltage dependence of the block decreased with an increase of polyamine charge; the mean $z\delta$ values for Put^{2+}, Spd^{3+} and Spm^{4+} were 1.33, 1.24 and 1.04, respectively. However, the value of z, which is a measure of the total charge transported across the entire pore upon establishment and relief of the block, on the contrary shows a moderate increase from 3.79 as an average for diamine Put^{2+} to 4.10 for the polyamines Spd^{3+} and Spm^{4+}. Remarkably, only for the tetravalent Spm^{4+} do the values of z and the nominal valence fit each other, whereas for the shorter Spd^{3+} and, especially, for Put^{2+} the value of z was clearly in excess of their actual valence, implying a movement of additional electrical charges across the channel pore.

As all the three polyamines tested acted as permeable blockers, there was a tantalising possibility to test their blocking effect from the *trans*, i.e. vacuolar, side. Typical single channel current-voltage relationships obtained in the presence of different concentrations of either Put^{2+} or Spm^{4+} at the vacuolar side are presented in Fig. 5a, b and relative currents (in the presence of blocker to control) as a function of membrane voltage are plotted in Fig. 5c, d. Firstly, it can be seen that the block was relieved at high negative potentials, and secondly, the voltage dependence of the block relief was valence dependent, being much steeper in the case of tetravalent Spm^{4+} compared to divalent Put^{2+} (Fig. 5c, d). Fitted parameters of the voltage-dependent block by vacuolar Put^{2+} and Spm^{4+} are collected in Table 1. The binding affinity at zero voltage for Spm^{4+} was within a range of

Table 1 Parameters of the SV channel voltage-dependent block by cytosolic and vacuolar polyamines

Concentration (10^{-3} M)	Rate constants at zero voltage			Valence and electrical distance		
	$k_1(0)$ (10^6 M^{-1})	$k_2(0)$	$K_d(0)$ (10^{-6} M)	z	δ	$z\delta$
Cytosolic[a]						
Putrescine						
0.1	0.07 ± 0.042	110 ± 46	2046 ± 446	3.87 ± 0.26	0.36 ± 0.03	1.37 ± 0.13
0.3	0.06 ± 0.034	131 ± 50	2382 ± 339	3.95 ± 0.22	0.35 ± 0.04	1.39 ± 0.23
1.0	0.05 ± 0.008	129 ± 15	2936 ± 189	3.76 ± 0.06	0.34 ± 0.01	1.29 ± 0.04
3.0	0.02 ± 0.009	82 ± 22	3910 ± 511	3.62 ± 0.10	0.34 ± 0.00	1.23 ± 0.03
10.0	0.02 ± 0.007	123 ± 43	5183 ± 223	3.74 ± 0.22	0.36 ± 0.05	1.38 ± 0.26
Spermidine						
0.03	0.46 ± 0.08	154 ± 59	346 ± 108	4.02 ± 0.01	0.29 ± 0.02	1.12 ± 0.09
0.10	0.53 ± 0.16	198 ± 36	450 ± 72	4.18 ± 0.03	0.30 ± 0.02	1.19 ± 0.10
0.30	0.50 ± 0.11	348 ± 106	706 ± 164	4.08 ± 0.07	0.32 ± 0.02	1.31 ± 0.06
1.0	0.60 ± 0.21	555 ± 151	1328 ± 401	4.11 ± 0.01	0.32 ± 0.01	1.33 ± 0.05
Spermine						
0.003	3.99 ± 0.42	120 ± 4.5	30.6 ± 2.3	4.02 ± 0.30	0.24 ± 0.04	0.95 ± 0.07
0.010	3.84 ± 1.32	190 ± 56	49.5 ± 11.3	4.17 ± 0.16	0.28 ± 0.02	1.20 ± 0.10
0.030	7.02 ± 2.48	431 ± 121	65.6 ± 6.6	4.06 ± 0.25	0.24 ± 0.03	0.97 ± 0.12
0.100	26.5 ± 5.86	2761 ± 563	105.6 ± 5.3	4.15 ± 0.23	0.25 ± 0.03	1.04 ± 0.16
Vacuolar						
Putrescine[b]						
1.0	0.009 ± .000	76 ± 7	8324 ± 563	1.92 ± 0.11	0.24 ± 0.02	0.46 ± 0.05
3.0	0.015 ± .003	129 ± 25	8534 ± 209	1.93 ± 0.01	0.21 ± 0.01	0.41 ± 0.03
10.0	0.012 ± .005	140 ± 60	12051 ± 35	1.86 ± 0.22	0.21 ± 0.00	0.39 ± 0.05
Spermine[a]						
0.010	3.95 ± 0.67	251 ± 75	65.0 ± 21.1	3.28 ± 0.19	0.12 ± 0.02	0.39 ± 0.08
0.030	19.9 ± 11.5	1751 ± 837	53.0 ± 2.0	3.73 ± 0.19	0.13 ± 0.03	0.47 ± 0.03
0.100	68.2 ± 30.7	5540 ± 2580	75.8 ± 5.0	3.76 ± 0.21	0.09 ± 0.01	0.32 ± 0.01

[a] Each parameter value (mean ± SD) is a result of 3–4 separate determinations
[b] Each parameter value (mean ± SD) is a result of 2 separate determinations

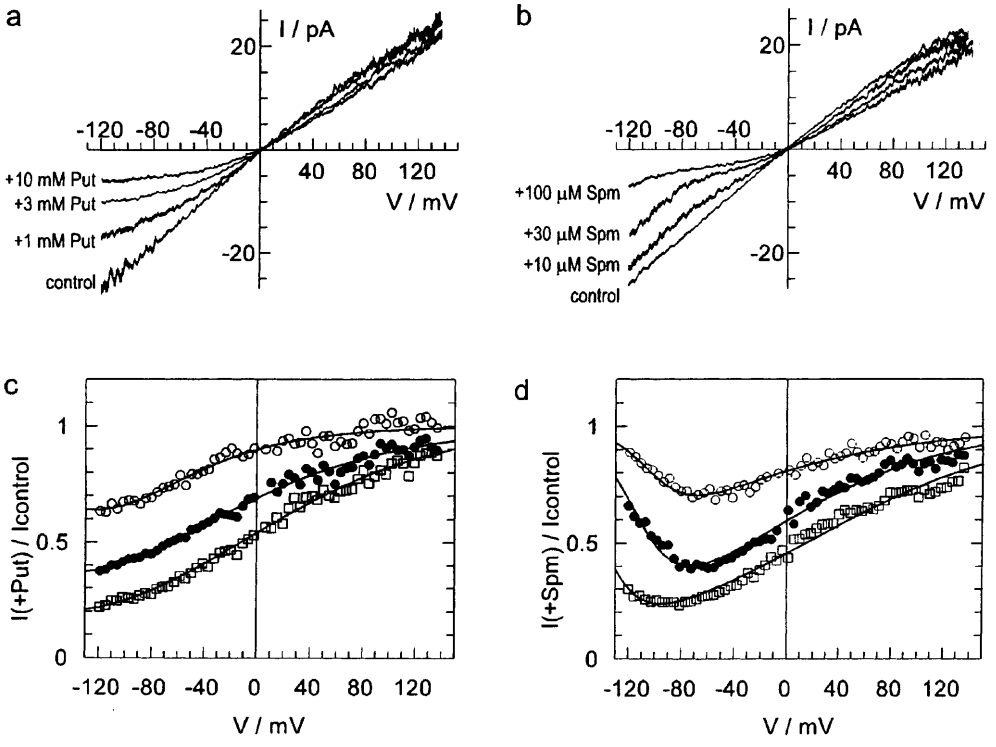

Fig. 5 Voltage-dependent block of the open SV channel current by vacuolar polyamines, putrescine, Put (**a**, **c**) and spermine, Spm (**b**, **d**). **a**, **b** Single channel current-voltage relationships; number of averages for controls in **a** and **b** was 35 and 77, respectively; for other curves: Put, 1 mM (n = 27), 3 mM (n = 43) and 10 mM (n = 32); Spm, 10 µM (n = 41), 30 µM (n = 38) and 100 µM (n = 51). **c**, **d** Corresponding relative currents; number of points was reduced five times by substitutive average. Symbols: **c** 1 mM Put (*open circles*), 3 mM Put (*filled circles*), 10 mM Put (*squares*); **d** 10 µM Spm (*open circles*), 30 µM Spm (*filled circles*), 100 µM Spm (*squares*). Data points were fitted to Eq. (3) with a variable z

values obtained at corresponding Spm^{4+} concentrations applied to the cytosolic side, whereas Put^{2+} displayed 2.3–2.8 times lower affinity compared to that for the cytosolic application. It appears that polyamines traversed much shorter electrical distances on their way to the binding site from the vacuolar surface compared to that from the cytosolic one. Whilst an approximately equal charge ($z\delta$), 0.42 and 0.39 as an average for Put^{2+} and Spm^{4+}, was moved into the pore upon blocking, the total charge moved across the entire pore differed roughly by a factor of two, z = 1.90 and 3.59, approaching the actual valence of Put^{2+} and Spm^{4+}, respectively.

Discussion

Calibre of the channel pore and comparison with other channels

Our results (Fig. 2) clearly show that the SV channel is permeable for TMA^+ but not measurably permeable for TEA^+. Firstly, when quaternary ammonium (QA) ions were applied from cytosolic side, the permeability for TMA^+ was evidenced by an upturn of the relative current at high positive voltages, indicating removal of TMA^+ to the vacuolar side. Such a relief of block was not observed with TEA^+ (Fig. 2b). Secondly, consistent with TMA^+ permeability, the channel was also transiently blocked by TMA^+ applied to the vacuolar side. On the other hand, TEA^+, being a more efficient blocker compared to TMA^+ when applied to the cytosolic side [$K_d(0) \sim 12$ mM], was completely inefficient from the vacuolar one. Hence, the binding site was accessible for TEA^+ only from the cytosolic side.

Therefore, we can conclude that the diameter of the channel pore at its narrowest cross-section exceeds the diameter of TMA^+ (~5.5 Å) but is smaller than that of TEA^+ (~8 Å). Long linear polyamines with a thickness in the extended conformation of ≤4 Å are all permeable, as evidenced by a relief of block at high potentials of either sign (Figs. 4 and 5). Molecular simulations have shown that putrescine and spermidine are both rigid, with a distance between N-termini fixed at 7 Å and ~9 Å, respectively, whereas spermine is highly flexible, so in the bend-over conformation the terminal N-atoms could come as close as 6 Å each to other (Weiger et al. 1998). Although we could not rule out the existence of alternative orientations of different polyamines within the channel pore, because of the gradual change of the voltage dependence of the block from Put^{2+} through Spd^{3+} to Spm^{4+} (Table 1) it is more likely that all three polyamines block and permeate the channel in the extended conformation aligned roughly parallel to the pore axis.

It appears from our data that purely sterical considerations could not account for the selective permeation of the SV channel. Indeed, $Tris^+$, which has a cross-section area formally 3% larger than that of TEA^+ (Coronado and Miller 1982), is nevertheless permeable (Fig. 3). In the case of $Tris^+$, terminal groups (three hydroxyls and/or the amino group) could transiently form the hydrogen bonds with the acceptor groups (possibly carboxyls) of the selectivity filter, thus reducing the effective ion size (Hille 1992). For example, in the

axon K^+ channel, tetrakis, a hydroxylated derivative of TEA^+, could squeeze twice as far as the smaller TEA^+ along the voltage drop (French and Shoukimas 1985). Similarly, $Tris^+$ readily permeated across the sarcoplasmic reticulum (SR) Ca^{2+} release channel, yet TEA^+ and even the much smaller (in either orientation) TMA^+ did not carry any significant current (Tinker and Williams 1993). It should be noted here that, in contrast to other authors, who defined the absolute and/or relative channel permeability for different ammonium derivatives, we simply tested whether the given organic cation could or could not pass, based on the presence or absence of the block relief at large membrane potentials. Relative as well as absolute permeability of at least some blocking cations is impeded by high energy barrier(s) rather than by simple ion sieving. A large voltage could simply help low permeant ions, for instance Na^+ in a K^+ channel, to overcome the high energy barrier imposed by the selectivity filter (French and Shoukimas 1985). However, in addition, the possibility that at large field strengths the selectivity filter conformation might show some degree of "give", thus allowing larger ions to permeate, should be kept in mind. Trimethylammonium derivatives as well as the parent TMA^+ could pass the SR Ca^{2+} release channel only when large (>60 mV) depolarising potentials were applied (Tinker and Williams 1995). To reveal the cytosolic TMA^+ permeability across the SV channel pore, we have had to extend the voltage range to $+180$ mV (Fig. 2b), as up to $+140$ mV the deviation from impermeable blocker behaviour was marginal. At moderate potentials (≤ 80 mV) the permeability of TMA^+ across the SV channel pore is negligibly small (Gambale et al. 1996).

The SV channel of higher plant vacuoles is a cation channel poorly selecting among mono- and divalent ions (Pantoja et al. 1992; Amodeo et al. 1994; Ward and Schroeder 1994). It has a peculiar pharmacological pattern, sensitivity to unspecific cation transport blockers, but also to charibdotoxin and tubocurarine, thought to be specific blockers of Ca^{2+}-activated maxi-K^+ and acetylcholine receptor (AchR) channels, respectively (Weiser and Bentrup 1993), and to a variety of anion transport blockers (Hedrich and Kurkdjian 1988). Therefore, the relation of the SV channel to the existing ion channel families could not be drawn easily. For comparative purposes we have considered known Ca^{2+}-permeable channels. The dimensions of the narrowest constriction in these channels was estimated using low permeable organic cations. Resulting minimal cross-sections of the selectivity filter ranged from 5.5 Å for a dihydropyridine-sensitive Ca^{2+} channel and a wild-type NMDA receptor through 5.8–6.5 Å for different cGMP-gated channels up to 7.0–7.6 Å for AchR and large conductance SR Ca^{2+} channels (Hille 1992; Goulding et al. 1993; Tinker and Williams 1993; Nutter and Adams 1995; Wollmuth et al. 1996), compared to our estimate of between 5.5 and 8 Å for the SV channel. The minimal diameter of about 7 Å is at the upper limit, allowing selective permeability for small inorganic cations, as it approaches the diameter of cation covered by the first hydration shell. The dehydration per se in selected cases may exert severe limits on the ion conductance. Particularly, Mg^{2+} (diameter with the first hydrated shell of 7 Å) holds water molecules >1000 times longer than Ca^{2+}, so if the conductance is limited by dehydration, an equivalent electric current for Mg^{2+} of only 40 fA will result. Consequently, voltage-dependent Ca^{2+} channels and NMDA receptors are not measurably permeable for Mg^{2+} (Nowak et al. 1984; Hille 1992), whereas AchR and SR Ca^{2+} release channels conduct Mg^{2+} (Adams and Nutter 1992; Tinker et al. 1992). Previously we have reported a high conductance of the SV channel for Mg^{2+} (Pottosin et al. 1997); hence, a diameter of the selectivity filter of about 7 Å, lying in the range indicated by QA ions, should be considered.

Interpretation of the voltage-dependent block of the SV channel by internal and external cations

The block of the SV channel by organic cations applied to the cytosolic side of the membrane strongly depends on the voltage. At the same time, the apparent electrical distance (δ) for all cations tested never exceeded unity, albeit approaching it in the case of quaternary ammonium ions. The block by permeable cations, with a notable exception of spermine, was nevertheless anomalously strong, as the voltage dependence of block relief at high membrane potentials indicated movement of additional charges in excess of the nominal valence for a given cation. Generally, extra charge, moving in the blocking reaction, may be provided by a second blocking cation, concerted movement of bulk ions or movable channel protein groups. However, to explain the strong voltage dependence of block relief, only the first two possibilities could be considered, as the extra charge has to leave the pore. Strong evidence for a concerted movement of blocking and bulk (K^+) cations was recently obtained on cloned inward-rectifier K^+ channels (Oliver et al. 1998; Pearson and Nichols 1998; Spassova and Lu 1998). Thus, the major portion of the voltage dependence might arise from the displacement of bulk ions rather than from that of the blocking ion, which helps to understand why sometimes the block by cations of different size had the same (strong) voltage dependence (Spassova and Lu 1998). Interestingly, in the present work on the SV channel, $z\delta$ values for permeable TMA^+ and impermeable TEA^+ were the same within experimental error, 0.96 and 0.94, respectively, indicating a common mechanism of block for larger and smaller QA ions. In principle, the concept of coupled movement of blocking and bulk ions might be expanded for the explanation of the strong voltage dependence of block relief in the case of a weakly permeable blocker. The block relief at large voltages implies that the blocking ion is accelerated by a strong electric field to such a rate that its removal becomes not limiting, hence the single channel current tends to approach the level of

the control. The residence times of blocking and bulk ions within the pore are therefore comparable in this voltage region, which means that movements of blocking and bulk cations are intrinsically coupled. This mechanism might serve as a plausible explanation for the anomalously high z values obtained in the case of block by cytosolic TMA^+ and $Tris^+$. Each of these blocking cations displaced approximately one charge across the whole voltage drop (or two charges by 50%) to plug the pore, and one more during block relief, in total roughly one extra charge (K^+ ion?).

The complex nature of block by cytosolic polyamines was overlooked in our previous study (Dobrovinskaya et al. 1999) owing to the presence of an additional blocking cation, $Tris^+$, in the experimental solutions. The blocking effect of $Tris^+$ had not been suspected previously and it has been widely utilised as a part of a pH-buffer system in experiments on the SV channel (Weiser and Bentrup 1993; Ward and Schroeder 1994; Schulz-Lessdorf and Hedrich 1995; Pottosin et al. 1997). The contribution of $Tris^+$ could be summarised as follows:

1. $Tris^+$ masked the variation of the parameters of the polyamine block voltage dependence with concentration (see Table 1).

2. $Tris^+$ and polyamines competed, leading to an apparently lower affinity of the polyamine block in the presence of $Tris^+$. At $+50$ mV in the presence of 28 mM $Tris^+$ the K_d for polyamines of 1680 μM (Put^{2+}), 190 μM (Spd^{3+}) and 30 μM (Spm^{4+}) were reported (Dobrovinskaya et al. 1999) compared to 234 μM, 54 μM and 9.7 μM in the absence of $Tris^+$, respectively (calculated from Table 1, this study). At $+50$ mV, 28 mM $Tris^+$ blocked 2/3 of the SV channel current (apparent $K_{d(Tris)} = 14.0$ mM, Fig. 3a, c). Assuming that the SV channel could handle either one $Tris^+$ or one polyamine ion at a time (simple competitive binding), the apparent binding constant for polyamine in the presence of $Tris^+$, $K_{d(PA)}^* = K_{d(PA)} \times (1 + [Tris^+]/K_{d(Tris)})$. This yields K_d^* of 702 μM, 162 μM and 29 μM for Put^{2+}, Spd^{3+} and Spm^{4+}, respectively. Only the K_d^* value for the block by Spm^{4+} accurately fits the prediction of a simple competitive scheme.

3. The voltage dependence of the polyamine block in the presence of $Tris^+$ was underestimated. For Spm^{4+}, Spd^{3+} and Put^{2+}, $z\delta$ values between 0.8 and 0.9 were reported previously (Dobrovinskaya et al. 1999) compared to average values of 1.04, 1.24 and 1.33, respectively (Table 1, this study). Previously we have estimated the length of the voltage drop within the channel pore under the assumption that the block is caused by a single polyamine ion with leading end fixed at a common position. The reverse dependence of $z\delta$ on the polyamine charge invalidates this assumption.

4. The most striking feature of the block by cytosolic polyamines revealed upon removal of $Tris^+$ from experimental solutions was its multi-ion nature in the case of shorter polyamines, which is manifested by a valence of block (z) higher than the actual valence of the blocking cation.

The extra charge moved across the entire pore decreased from ~2 for Put^{2+} to ~1 for Spd^{3+} and vanished in the case of Spm^{4+} (Table 1). Thus, first Spm^{4+} appears to saturate the binding sites of the cytosolic domain of the pore; hence a simple one-to-one block, with no extra charge movement, resulted, which is also consistent with the simple mechanism of competition with $Tris^+$. However, rate constants for Spm^{4+} binding at zero voltage strongly depended on the concentration (Table 1), resulting in a gradual shift of the voltage dependence of the block along the potential axis. This shift could be attributed to the short-range electrostatic repulsion between Spm^{4+} ions, occupying the pore, rather than to the change of membrane surface potential due to an increase of bulk polyamine moiety, as the direction of the shift was opposite to that expected in the latter case. Additional Spm^{4+} ion(s), however, must reside close to the vacuolar surface and outside the voltage drop across the pore, because no appreciable change of slope parameters (z and δ) was observed with the increase of concentration (Table 1). Hence, it could be concluded that the cytosolic voltage-sensing domain of the pore could handle one Spm^{4+} at the same time. The physical distance of the cytosolic fraction of the voltage drop across the pore could be approximated by the length of the relaxed conformation of a single Spm^{4+}, 13.8 Å as an upper limit (Weiger et al. 1998). It remains to estimate the extent of the vacuolar fraction of the voltage drop.

The voltage dependence of the SV channel block by organic cations tested was asymmetric, with the $z\delta$ value being larger by a factor of 2.3–3.3 for cytosolic compared to vacuolar application. Binding of $Tris^+$ and TMA^+ took place at an electrical distance of about 30% from the vacuolar surface, arguing for a common binding site. In the case of Put^{2+} and Spm^{4+}, the average electrical distance was about 20% and 10%, respectively (Table 1). The latter reflects the mean distance traversed by charged groups of a long polycation within the voltage drop, hence providing information on the approximate length of this region. Our data evidenced that the vacuolar part of the pore is likely shorter than the cytosolic one, both in terms of electrical and physical distances. According to the z values obtained for Put^{2+} and Spm^{4+} upon application to the vacuolar side, which approached their actual valence, the pore could handle one polyamine ion at a time. Based on approximately equal $z\delta$ values for Spm^{4+} and Put^{2+}, 0.39 and 0.42 as an average, the third and fourth amino groups of Spm^{4+} did not contribute significantly to the block voltage dependence, hence are outside the voltage drop. Given that either one or both amino groups of Put^{2+} could traverse the voltage drop from the vacuolar side, the electrical distance traversed by the leading amino group may not exceed $z\delta$ (0.42) but it is larger or equal to δ (0.22). The 30% binding site revealed by TMA^+ and $Tris^+$ is in the middle between the upper and lower estimates for the

electrical distance to the polyamine-binding site. Therefore, it is reasonable to propose that all organic amines share the same binding site, accessible from the vacuolar side of the pore. Providing the vacuolar voltage-sensing region of the pore may accommodate up to two amino groups of either Put^{2+} or Spm^{4+}, its physical distance would be roughly the length of a single Put^{2+} or half of a Spm^{4+} ion (~7 Å). Added to the length of the cytosolic region, the total voltage drop across the pore would occur within a distance < 21 Å. This is a reasonable estimate, keeping in mind that a longer pore will have a higher resistance. Approximating the pore in the SV channel by a 20 Å-long and 8 Å-wide (diameter of TEA^+) cylinder, filled by 0.1 M KCl, resulted in a limiting conductance of 206 pS (resistance of 4.85 GΩ). The experimentally defined value of 208 ± 8 pS ($n = 32$) already approached the theoretical ceiling imposed by diffusion limitations. It should be mentioned that the previously reported lower unitary conductance values for SV channels (for review, see Schulz-Lessdorf and Hedrich 1995) seem to be an underestimate. All these values have been obtained in the presence of high concentrations of Ca^{2+}, Mg^{2+} and/or $Tris^+$, which reduced the single channel current (Gambale et al. 1996; this paper).

Our data on the voltage-dependent block of plant vacuolar large conductance SV channels are consistent with the view that its selectivity filter is located asymmetrically, closer to the vacuolar than to the cytosolic end of the pore. The cytosolic part of the pore could adopt several ions at a time; the relative contributions of the blocking and permeant ions to the observed voltage dependence of the block remains to be elucidated.

Acknowledgements This work was funded by CONACyT grants 3735P-N9607 and 29473N to I.I.P. The authors wish to thank Dr. Sanchez Chapula for the critical reading of the manuscript.

References

Adams DJ, Nutter TJ (1992) Calcium permeability and modulation of nicotinic acetylcholine receptor-channels in rat parasympathetic neurons. J Physiol (Paris) 86: 67–76

Allen GJ, Sanders D, Gradmann D (1998) Calcium-potassium selectivity: kinetic analysis of current-voltage relationships of the open, slowly activating channel in the vacuolar membrane of *Vicia faba* guard cells. Planta 204: 528–541

Amodeo G, Escobar A, Zeiger E (1994) A cationic channel in the guard cell tonoplast of *Allium cepa*. Plant Physiol 105: 999–1006

Coronado R, Miller C (1982) Conduction and block by organic cations in a K^+-selective channel from sarcoplasmic reticulum incorporated into planar phospholipid bilayers. J Gen Physiol 79: 529–547

Czempinski K, Zimmermann S, Erhardt T, Müller-Röber B (1997) New structure and function in plant K^+ channels: KCO1, an outward rectifier with a steep Ca^{2+}-dependency. EMBO J 16: 2565–2575

Dobrovinskaya OR, Muñiz J, Pottosin II (1999) Inhibition of vacuolar channels by polyamines. J Membr Biol 167: 127–140

Dreyer I, Antunes S, Hoshi T, Müller-Röber B, Palme K, Pongs O, Reintanz B, Hedrich R (1997) Plant K^+ channel α-subunits assemble indiscriminately. Biophys J 72: 2143–2150

French RJ, Shoukimas JJ (1985) An ion's view of the potassium channel. The structure of the permeation pathway as sensed by a variety of blocking ions. J Gen Physiol 85: 669–698

Gambale F, Bregante M, Stragapede F, Cantu AM (1996) Ionic channels of the sugar beet tonoplast are regulated by a multi-ion single-file permeation mechanism. J Membr Biol 154: 69–79

Goulding EH, Tibbs GR, Liu D, Siegelbaum SA (1993) Role of H5 domain in determining pore diameter and ion permeation through nucleotide-gated channels. Nature 364: 61–64

Hedrich R, Kurkdjian A (1988) Characterization of an anion-permeable channel from sugar beet vacuole: Effect of inhibitors. EMBO J 7: 3661–3666

Hedrich R, Neher E (1987) Cytoplasmic calcium regulates voltage-dependent ion channels in plant vacuoles. Nature 329: 833–835

Hedrich R, Barbier-Brygoo H, Felle H, Fluegge UI, Luettge U, Maathuis FJM, Marx S, Prins HBA, Raschke K, Schnabl H, Schroeder JI, Struve I, Taiz L, Zeigler P (1988) General mechanisms for solute transport across the tonoplast of plant vacuoles: a patch-clamp survey of ion channels and proton pumps. Bot Acta 101: 7–13

Hedrich R, Moran O, Conti E, Busch H, Becker D, Gambale F, Dreyer I, Küch A, Neuwinger K, Palme K (1995) Inward rectifier potassium channels in plants differ from their animal counterparts in response to voltage and channel modualtors. Eur Biophys J 24: 107–115

Hille B (1992) Ionic channels of excitable membranes, 2nd edn. Sinauer, Sunderland, Mass

Miller C (1982) Bis-quaternary ammonium blockers as structural probes of the sarcoplasmic reticulum K^+ channel. J Gen Physiol 79: 869–891

Nowak I, Bregestovski P, Ascher P, Herbert A, Prochiantz A (1984) Magnesium gates glutamate-activated channels in mouse central neurones. Nature 307: 462–465

Nutter TJ, Adams DJ (1995) Monovalent and divalent cation permeability and block of neuronal nicotinic receptor channels in rat parasympathetic ganglia. J Gen Physiol 105: 701–723

Oliver D, Hahn H, Antz C, Ruppersber JP, Fakler B (1998) Interaction of permeant and blocking ions in cloned inward-rectifier K^+ channels. Biophys J 74: 2318–2326

Pantoja O, Gelli A, Blumwald E (1992) Voltage-dependent calcium channels in plant vacuoles. Science 255: 1567–1570

Pearson WL, Nichols CG (1998) Block of the Kir2.1 channel pore by alkylamine analogues of endogenous polyamines. J Gen Physiol 112: 351–363

Pottosin II, Tikhonova LI, Hedrich R, Schönknecht G (1997) Slowly activating vacuolar channels can not mediate Ca^{2+}-induced Ca^{2+}-release. Plant J 12: 1387–1398

Pottosin II, Muñiz J, Dobrovinskaya OR (1999) Characterization of the selectivity filter in calcium-permeable channel of plant vacuoles. Biophys J 76: A378

Schulz-Lessdorf B, Hedrich R (1995) Protons and calcium modulate SV-type channels in the vacuolar-lysosomal compartment. Channel interaction with calmodulin inhibitors. Planta 197: 655–671

Spassova M, Lu Z (1998) Coupled ion movement underlies rectification in an inward-rectifier K^+ channel. J Gen Physiol 112: 211–221

Tinker A, Williams AJ (1993) Probing the structure of the conduction pathway of the sheep cardiac sarcoplasmic reticulum calcium-release channel with permeant and impermeant organic cations. J Gen Physiol 102: 1107–1129

Tinker A, Williams AJ (1995) Measuring the length of the pore in the sheep cardiac sarcoplasmic reticulum calcium-release channel using related trimethylammonium ions as molecular calipers. Biophys J 68: 111–120

Tinker A, Lindsay ARG, Williams AJ (1992) A model for ionic conduction in the ryanodine receptor channel of sheep cardiac muscle sarcoplasmic reticulum. J Gen Physiol 100: 495–517

Villarroel A, Alvarez O, Oberhauser A, Latorre R (1988) Probing a Ca^{2+}-activated K^+ channel with quaternary ammonium ions. Pflügers Arch Eur J Physiol 413: 118–126

Ward JM, Schroeder JM (1994) Calcium-activated K^+ channels and calcium-induced calcium release by slow vacuolar ion channels in guard cell vacuoles implicated in the control of stomatal closure. Plant Cell 6: 669–683

Weiger TM, Langer T, Hermann A (1998) External action of di- and polyamines on maxi calcium-activated potassium channels: an electrophysiological and molecular modeling study. Biophys J 74: 722–730

Weiser T, Bentrup F-W (1993) Pharmacology of the SV channel in the vacuolar membrane of *Chenopodium rubrum* suspension cells. J Membr Biol 136: 43–54

Wollmuth LP, Kuner T, Seeburg PH, Sakmann B (1996) Differential contribution of the NR1- and NR2-subunits to the selectivity filter of recombinant NMDA receptor channels. J Physiol (Lond) 491: 779–797

Woodhull AM (1973) Ionic block of sodium channels in nerve. J Gen Physiol 61: 687–708